Anisotropy and Molecular Rotation in Resonant Low-Energy Dissociative Recombination

S. Novotny,[1] H. Rubinstein,[2] H. Buhr,[1,2] O. Novotný,[1] J. Hoffmann,[1] M. B. Mendes,[1] D. A. Orlov,[1] C. Krantz,[1] M. H. Berg,[1] M. Froese,[1] A. S. Jaroshevich,[3] B. Jordon-Thaden,[1] M. Lange,[1] M. Lestinsky,[1] A. Petrignani,[1] D. Shafir,[2] D. Zajfman,[2] D. Schwalm,[1,2] and A. Wolf[1]

[1]*Max-Planck-Institut für Kernphysik, 69117 Heidelberg, Germany*
[2]*Department of Particle Physics, Weizmann Institute of Science, Rehovot 76100, Israel*
[3]*Institute of Semiconductor Physics, 630090 Novosibirsk, Russia*

(Received 21 December 2007; published 14 May 2008)

Angular fragment distributions from the dissociative recombination (DR) of HD^+ were measured with well directed monochromatic low-energy electrons over a dense grid of collision energies from 7 to 35 meV, where pronounced rovibrational Feshbach resonances occur. Significant higher-order anisotropies are found in the distributions, whose size varies along energy in a partial correlation with the relative DR rate from fast-rotating molecules. This may indicate a breakdown of the nonrotation assumption so far applied to predict angular DR fragment distributions.

DOI: 10.1103/PhysRevLett.100.193201 PACS numbers: 34.80.Lx, 34.80.Ht

Positively charged molecules can be fragmented efficiently by low-energy electron impact at collision energies down to the sub-eV range in the process of dissociative recombination (DR) [1]. This reaction attracts strong interest in the modeling of the chemical networks in cold and dilute ionized media such as interstellar clouds [2], atmospheric layers [3], and industrial plasmas [4]. It is driven by the formation of intermediate neutral compound states, in which the incident electron is captured following resonant energy exchange with the cation, and which then dissociate into neutral product channels reached via excited potential surfaces.

Rovibrational Feshbach resonances were recognized to play an important role at low electron energies in the DR [5] as well as in the related process of dissociative electron attachment (DEA), an efficient destruction channel of neutral molecules by low-energy electron impact [6,7]. They reflect the energy exchange of the incident electron with the nuclear motion, in contrast to the one within the electronic system alone. Thus, in the *direct* mechanism [5] of DR purely electronic energy exchange forms a neutral, doubly excited potential surface unstable against dissociation. In the *indirect* mechanism [5] a rovibrationally excited neutral Rydberg state is formed with the initial bound electronic state of the ion as a core and then predissociated by often the same doubly excited surface. These mechanisms interfere with each other as pathways of comparable strength, creating a rich structure of rovibrational Feshbach resonances in the low-energy DR cross section [8]. For some key systems the importance of the nonadiabatic coupling mechanisms between electronic and nuclear motion leading to *indirect* DR was considerably underestimated until recent studies [9,10]. Under practical aspects, the rates of these processes at low electron energies become particularly sensitive to the rovibrational temperature of the colliding molecules [6,8].

So far, molecular fragmentation by slow electrons has mainly been investigated through rate measurements. Event-by-event counting experiments on DR between molecular ions of thermal rovibrational energies (temperature $\sim$300 K) and nearly monochromatic electrons at energies down to a few meV used fast cation beams in ion storage rings overlapped with electron beams at nearly matched velocities [11]. In the present experiment on the deuterated hydrogen molecular ion HD^+ we for the first time analyze the product kinematics associated with these resonances at energies of $\sim$10–80 meV. Both the energy release and the fragment angular distribution are obtained by applying well directed, nearly monoenergetic incident electrons on a dense energy grid. The measurements are made possible by a unique twin-electron-beam arrangement recently introduced in our ion storage ring, which allows us to perform fragment imaging under stable ion beam conditions for variable low electron-collision energies. In addition, a new photocathode electron source is used to generate an electron beam at transverse temperatures of only $\sim$0.5 meV [12]. From the fragment energy release, we characterize how strongly various initial rotational levels of HD^+ contribute to the DR resonance structures observed as a function of the electron energy. From the fragment angular distributions, we determine the differential rates as a function of the product angle with respect to the incident electron direction. They reveal significant variations of the anisotropy as a function of the electron impact energy and thereby open up a new observational window on rovibrational Feshbach resonances as a doorway for molecular fragmentation by cold electrons.

The species HD^+ has found much attention in precision studies of DR at ion storage rings [13] as its simple structure particularly favors an accurate theoretical description. Stored HD^+ ion beams were shown to vibrationally relax within $<$0.5 s [14] by infrared emission thanks to

the isotopic asymmetry. Hence, the initial energy above the HD^+ ground state is given by that of the colliding electron plus the ionic rotational excitation not far from a blackbody equilibrium at the 300-K ambient temperature. The DR at low collision energy E is then due to essentially a single route, the doubly excited neutral HD configuration $(2p\sigma_u)^2$ of $^1\Sigma_g^+$ symmetry. Earlier energy scans of the HD^+ DR cross section at storage rings [13] found it to vary at $E \lesssim 0.1$ eV by large factors (up to >4) with structures only a few meV wide superimposed on a general E^{-1} slope. This is theoretically understood [8,15] as a result of numerous rovibrational HD Feshbach resonances predissociated by the $(2p\sigma_u)^2$ state and interfering with *direct* DR via the same route. The resonances reflect [8], among other quantum numbers, the initial HD^+ rotational level J, although a detailed assignment of the observed patterns is still missing. A dominance of the electronic d partial wave is predicted for these collisions [15]. Other storage-ring measurements [16] showed that the final atomic product channels in these low-energy collisions are $H(n') + D(n)$ or $D(n') + H(n)$ with $n' = 1$ and $n = 2$ only.

The experiment uses the test-storage-ring (TSR) of the Max-Planck-Institut für Kernphysik, Heidelberg, Germany, with HD^+ ions injected and stored at 1.44 MeV kinetic energy, the typical circulating currents being ~10 nA. Electron beams copropagating with the stored ions in straight sections of the ring are used for phase-space cooling of the circulating beam and for low-energy collision measurements. The electron beam velocity is matched to that of the ion beam at a laboratory acceleration voltage of ~260 V. Detuning the acceleration voltage from its matching value, quasimonoenergetic electron-ion interactions can be realized. The collision energies lie close to a value E_d determined by the detuning, the monochromaticity being limited by the thermal electron velocities.

The new twin-electron-beam technique uses a separate electron-target section (ETS) [17] in the TSR, where the electron-collision energy can be independently tuned while the electron cooler continuously maintains a circulating HD^+ beam of $\lesssim 0.1$ mrad root-mean-square (rms) divergence and <1 mm rms diameter. The electron cooler of the TSR yields an electron beam with a density of 1.6×10^7 cm^{-3} and thermal electron energies of $kT_\perp \sim 10.0$ meV and $kT_\parallel \sim 0.1$ meV transverse and parallel to the beam direction, respectively, in its comoving reference frame. Its constant acceleration voltage precisely defines the energy of the stored ion beam. In the ETS, the GaAs photocathode source [12] yields an electron beam with thermal energies of $kT_\perp \sim 0.5$ meV and $kT_\parallel \sim 0.03$ meV; it was run at electron densities n_e of 0.63×10^6 cm^{-3} and 1.27×10^6 cm^{-3}. The temperatures were derived from the sharpest structures [12] observed in the energy-dependent DR rate. For some data, a thermionic cathode was used in the ETS, yielding $kT_\perp \sim 2.0$ meV and $kT_\parallel \sim 0.045$ meV at $n_e = 2.79 \times 10^6$ cm^{-3}.

Events caused by DR are identified through the quasisimultaneous arrival of two neutral fragments at counting or imaging detectors downstream of the ETS. The procedures are similar to earlier measurements on cross sections [13] and fragment imaging [16,18,19] for DR. For high resolution fragment imaging, a new neutral beam line with an 80-mm diameter multichannel-plate (MCP) detector at $\bar{s} = 12.24$ m distance from the center of the ETS was used. It is read out by a CCD camera viewing an attached phosphor screen, recording separate images of individual neutral-hit events [20] at a rate of up to 30 s^{-1}. The transverse distance D between the two neutral fragments of double hit events is extracted with a resolution of <100 μm. The differences between the fragment hit times for the high beam velocities applied here are too small compared with the experimental time resolution to yield useful information on the event geometries and therefore not read out. A 5×5 cm^2, energy resolving surface barrier detector was temporarily placed ~0.5 m in front of the MCP to measure the total DR rate [13].

Over many repeated cycles, the HD^+ ions were injected within ~30 μs only and electron collisions were then studied over times of 7–17 s after injection, detuning the ETS to the desired collision energies $E_d \neq 0$. Reference imaging measurements at $E_d = 0$ were performed before and after this period in order to detect any rotational excitation of the HD^+ beam during the phase with $E_d \neq 0$ by changes in the fragment distance distributions $F(D)$. Both reference distributions were found identical within the accuracy, showing that any possible rotational excitation by the $E_d \neq 0$ electrons could be effectively cooled away by the ~10 times denser beam of the electron cooler. For measurements with the thermionic cathode the total storage time was 15 s and the ETS was operated continuously at $E_d \neq 0$ without affecting the ion beam quality.

The transverse distance D between the fragments is related through $D = s\delta_J \sin\theta$ [18] to their emission angle θ in the comoving frame relative to the beam axis, the maximum laboratory emission angle δ_J for HD^+ ions in the given initial rotational state J, and the distance s of the event from the detector. The related distributions $F(D)$ for the merged beams geometry [18] with $s_1 \leq s \leq s_2$ ($s_2 - s_1 = 1.3$ m) carry two essential items of information. First, the approach to zero at large D indicates the energy release of the reaction, the maximum in D being given by $s_2\delta_J$. Thus, a larger contribution of excited rotational levels to the DR rate can be identified through a higher end point of $F(D)$. Second, the functional dependence, especially at intermediate D, reflects the fragment angular distribution. Both properties (Fig. 1) were found to distinctly vary over as little as 2 meV in E_d.

In the analysis, we decompose the distribution $W(\theta)$ of fragment angles θ relative to the beam axis in the comov-

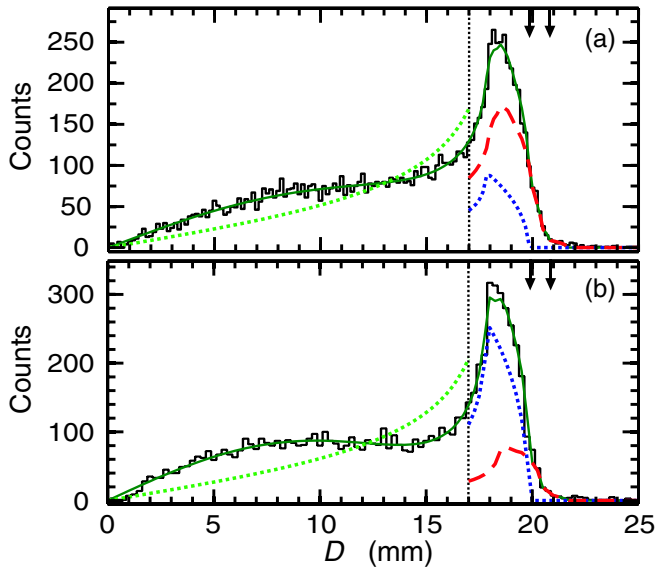

FIG. 1 (color online). Transverse distance distributions $F(D)$ for $E_d = 25$ meV (a) and $E_d = 27$ meV (b) with fits by Eq. (1) (solid line) requiring sizable contributions of Legendre polynomials of order $n = 2$ and 4. For comparison, the distributions expected for isotropic emission are indicated by dotted lines ($D < 17$ mm). For $D > 17$ mm the contributions to the fit from initial levels $J \leq 1$ (short-dashed) and $J \geq 2$ (long-dashed) are shown. Arrows indicate the maximum D values for $J = 1$ and 5, respectively.

ing frame into Legendre polynomials $P_n(\cos\theta)$, i.e., $W(\theta) = \sum_n a_n P_n(\cos\theta)$, with $a_0 = 1$ and anisotropy coefficients a_n for $n \geq 0$. This expansion yields corresponding terms $a_n F_{J,n}(D)$ in the transverse distance distribution $F(D)$ after averaging [18] over the event distances s, separately for each order n and each initial J with its related maximum emission angle δ_J. As the measured $F(D)$ do not allow us to determine individual sets of anisotropy coefficients for each J, we fitted the normalized distributions by

$$F(D) = \sum_J b_J \sum_n a_n F_{J,n}(D), \qquad (1)$$

where a_n represent the anisotropy coefficients averaged over all initial J levels and b_J the relative contributions of the initial ionic rotational states J to the total DR signal. Since events with θ and $\pi - \theta$ are not distinguished in the experiment, only even orders n occur in Eq. (1). The fits were performed by adjusting a_2, a_4, and b_J for $J \geq 0$, but setting $b_0 = b_1 = b_{01}/2$ to account for the small, experimentally unresolvable rotational energy difference between $J = 0$ and 1. Our excellent distance resolution does allow us (Fig. 1) to clearly distinguish the relative $J = 0$, 1 contribution b_{01} from the fraction $1 - b_{01}$ stemming from the higher rotational levels. Moreover, unlike previous DR experiments revealing only a_2 anisotropy coefficients [18,19], the present data clearly reveal the presence of the higher-order anisotropy coefficient a_4; coefficients of even higher order were found to be insignificant and omitted in the final analysis. The extracted rotationally averaged DR rate coefficient $\tilde{\alpha}(E_d)$ together with the low-J fraction b_{01} and the rotationally averaged anisotropy coefficients a_2 and a_4 are shown on Fig. 2. The scan of $\tilde{\alpha}(E_d)$ at the highest energy resolution realized so far reveals the three lowest-energy DR peaks [13], indicating a multicomponent array of rovibrational Feshbach resonances. From fragment imaging, we find that both the rotational contributions and the anisotropy parameters vary in similar resonant patterns; for example, in a region of E_d somewhat shifted from the main peak in $\tilde{\alpha}(E_d)$ low rotational levels ($J = 0$ and 1) of HD^+ yield the dominant fraction ($b_{01} \sim 0.8$) of the DR events. As a general trend, large low-J contributions coincide with peaks in the anisotropy coefficients, with the strongest variations occurring in a_4.

So far, the only available calculations on anisotropies in DR [21] are inspired by those for DEA [22] and apply the greatly simplifying axial-recoil (nonrotation) approximation [23]. In these calculations the angular dependence of the collision matrix element $T(\theta)$, related to the angular

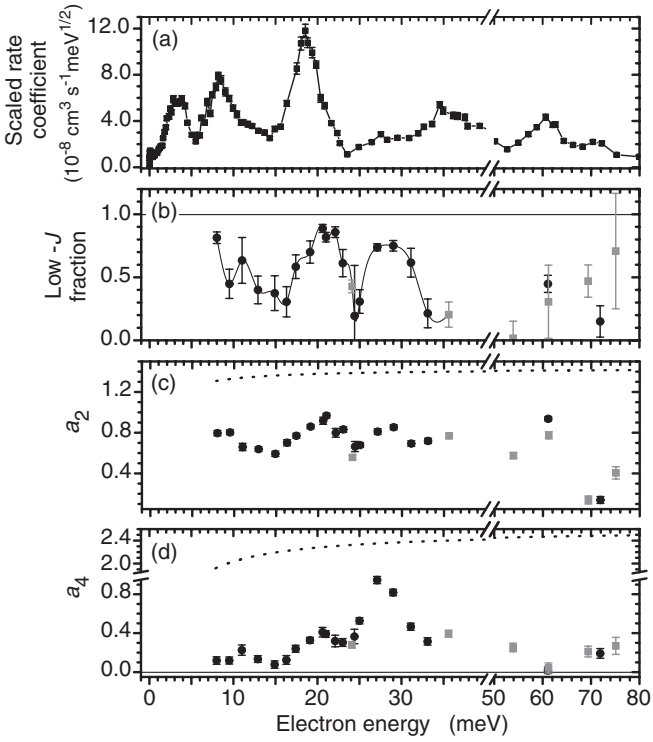

FIG. 2. (a) Scaled, rotationally averaged DR rate coefficient $\tilde{\alpha}(E_d)E_d^{1/2}$, (b) low-$J$ fraction b_{01} (symbols connected to guide the eye), and (c),(d) anisotropy coefficients a_2 and a_4 as functions of the detuning energy E_d. The photocathode was used except for the gray symbols indicating use of the thermionic cathode. The dotted lines indicate the values of $a_n = \chi_n(E_d)\tilde{a}_n$ for pure d symmetry of the transition matrix.

distribution by $W(\theta) \propto |T(\theta)|^2$, is determined by the electronic symmetries of the involved molecular configurations and the partial wave of the impinging electron [21,22]. For hydrogen molecular ions, a large dominance of the d partial wave is predicted [15] together with some s wave contributions [8]. A pure d wave implies according to Eq. (19) and Table I of Ref. [21] that $T(\theta)$ is proportional to the spherical harmonic $Y_{20}(\theta)$. The resulting angular distribution $|Y_{20}(\theta)|^2$ for strictly unidirectional electrons has anisotropy coefficients $\tilde{a}_2 = 10/7$ and $\tilde{a}_4 = 18/7$. The reduction of the anisotropy coefficients by the spread in incident electron directions is described by convolution factors $\chi_n(E_d) < 1$ which, however, at the present low transversal electron temperatures are calculated to deviate from unity by only <20% for $E_d > 7$ meV. Lines of $a_n = \chi_n(E_d)\tilde{a}_n$ for a pure d-type anisotropy are included in Figs. 2(c) and 2(d), showing that the measured anisotropy coefficients are by far smaller. Assuming the more general case of interfering s- and d-wave contributions with the amplitude of the latter given by c_2, the expected coefficient a_4 is modified to $\chi_4(E_d)\tilde{a}_4|c_2|^2$ (while a_2 also depends on the relative phase of the two contributions). Hence, relying on the axial-recoil approximation, $|c_2|^2$ is proportional to a_4 and can be read off directly from Fig. 2(d) to yield $|c_2|^2 < 0.5$ at maximum.

Our results indeed confirm a fourth-order anisotropy in the angular fragment distribution for the HD^+ DR with unidirectional low-energy electrons, as expected from the long-predicted dominance of the electronic d wave in this reaction [15]. However, analyzing the data within the axial-recoil approximation we find a rather small d-wave contribution with at least equally large s wave amplitudes, whose superposition varies strongly as the impact energies cross rovibrational Feshbach resonances. It should be noted that the axial-recoil approximation [22,23] to be valid requires steep dissociating potential surfaces as well as any Feshbach resonance lifetimes to be short compared to the molecular rotational period. Any deviations from these requirements will smear out the measured angular dependence, reduce the anisotropy coefficients as discussed, for example, for photodissociation [24], and introduce in $T(\theta)$ explicit influences of the nuclear rotational motion. Especially for the *indirect* DR involving rovibrational Feshbach resonances, sizable molecular rotation angles are expected during the resonance lifetimes. Thus, choosing 3 meV as the typical natural width for the observed structures, the mean resonance lifetimes are estimated to $\tau_r \sim 0.2$ ps. On the other hand, the relevant rotational period is given by the quantum number J' of the HD^+ ionic core in the resonant state and amounts to ~ 0.8 ps$/J'$. This indicates non-negligible rotation during τ_r even for the lowest J'. Describing the nuclear rotation in the resonant state, J' can generally differ from the initial J of the colliding HD^+ ion by as much as four units, considering d-wave coupling to be active [8]. Therefore, the observed degree of anisotropy probably reflects many details of the angular momentum exchange on the various Feshbach resonances, to be further explored by suitable fully rotational calculations. As a general trend, it can be assumed that the deduced relative contributions b_J also roughly characterize the range of J' for the resonances contributing to the DR signal. Indeed, the low-J fractions and the anisotropy parameters displayed in Fig. 2 show correlated variations with energy, which supports the conjecture of a growing loss of anisotropy and stronger deviations from the axial-recoil approximation as the molecular rotation increases.

For future theoretical approaches, a detailed dynamical picture appears more adequate for describing fragment anisotropies in DR than the simplifying assumptions made in their present theoretical treatment [21]. In particular on rovibrational Feshbach resonances, anisotropy studies elucidate the roles played by state symmetries and by the coupled quantum dynamics of electrons and nuclei in low-energy electron capture by molecules.

We thank C. H. Greene, I. F. Schneider, and F. O. Waffeu Tamo for very useful discussions. D. Schwalm acknowledges support by the Weizmann Institute through the Joseph Meyerhoff program. This work has been funded in part by the German Israeli Foundation for Scientific Research (GIF) under Contract No. I-707-55.7/2001.

[1] D. R. Bates, Adv. At. Mol. Opt. Phys. **34**, 427 (1994).
[2] J. Woodall *et al.*, Astron. Astrophys. **466**, 1197 (2007).
[3] S. L. Guberman, Science **278**, 1276 (1997).
[4] A. Bultel *et al.*, Phys. Plasmas **13**, 043502 (2006).
[5] J. N. Bardsley, J. Phys. B **1**, 365 (1968).
[6] H. Hotop *et al.*, Adv. At. Mol. Opt. Phys. **49**, 85 (2003).
[7] F. Martin *et al.*, Phys. Rev. Lett. **93**, 068101 (2004).
[8] I. F. Schneider *et al.*, J. Phys. B **30**, 2687 (1997).
[9] V. Kokoouline, C. H. Greene and B. D. Esry, Nature (London) **412**, 891 (2001).
[10] R. Čurík and C. H. Greene, Phys. Rev. Lett. **98**, 173201 (2007).
[11] M. Larsson, Annu. Rev. Phys. Chem. **48**, 151 (1997).
[12] D. A. Orlov *et al.*, J. Phys. Conf. Ser. **4**, 290 (2005).
[13] A. Al-Khalili *et al.*, Phys. Rev. A **68**, 042702 (2003).
[14] Z. Amitay *et al.*, Science **281**, 75 (1998).
[15] A. Giusti-Suzor, J. N. Bardsley, and C. Derkits, Phys. Rev. A **28**, 682 (1983).
[16] D. Zajfman *et al.*, Phys. Rev. Lett. **75**, 814 (1995).
[17] F. Sprenger *et al.*, Nucl. Instrum. Methods Phys. Res., Sect. A **532**, 298 (2004).
[18] Z. Amitay *et al.*, Phys. Rev. A **54**, 4032 (1996).
[19] J. Semaniak *et al.*, Phys. Rev. A **54**, R4617 (1996).
[20] I. Nevo *et al.*, Phys. Rev. A **76**, 022713 (2007).
[21] S. L. Guberman, J. Chem. Phys. **120**, 9509 (2004).
[22] T. F. O'Malley and H. S. Taylor, Phys. Rev. **176**, 207 (1968).
[23] R. N. Zare, J. Chem. Phys. **47**, 204 (1967).
[24] C. Jonah, J. Chem. Phys. **55**, 1915 (1971).